Title: Characteristic of slow growth in cell culture of adenovirus type 54 causing nationwide outbreak epidemic keratoconjunctivitis in Japan

Running Title: Slow propagation of adenovirus 54

Tomoko Tsukahara-Kawamura[1,2)], Nozomu Hanaoka[2)], Masami Konagaya[2)], Eiichi Uchio[1) *], Tsuguto Fujimoto[2)]

[1)] Department of Ophthalmology, Fukuoka University School of Medicine, 7-45-1 Nanakuma, Jonan-ku, Fukuoka 814-0180, Japan

[2)] Infectious Disease Surveillance Center, National Institute of Infectious Diseases, 1-23-1 Toyama, Shinjuku-ku, Tokyo 162-8640, Japan

***Corresponding author:** Eiichi Uchio, M.D., PhD.

Department of Ophthalmology, Fukuoka University School of Medicine, 7-45-1 Nanakuma, Jonan-ku, Fukuoka 814-0180, Japan,

Tel +81 92 801 1011

Fax +81 92 865 4445

E-mail: euchio@fukuoka-u.ac.jp

Abstract

Purpose: To characterize the virological features of adenovirus type 54 (Ad54) causing nationwide outbreak of severe epidemic keratoconjunctivitis (EKC) in Japan, we

comparatively analysed the viral propagation phenotype of Ad54 and other Ads: Ad type 37 (Ad37), 64 (Ad64), and 5 (Ad5), in A549 cells quantitatively.

Study Design: Laboratory investigation

Methods: We compared the growth rate of Ads using copy numbers and cytopathic effect observation during propagation in A549 cell lines. Expressions of mRNA of E1 gene were also calculated and compared. Phylogenetic analysis of the region, including putative promoter of E1 gene and E1 open reading frame (ORF), were performed.

Results: Increases in viral loads, growth rate, and viral propagation were slower for Ad54 than for other Ads. The expression level of the E1 gene per infected cell was lower for Ad54 than for other Ad types on post-infection day 1. Phylogenetic analysis of the E1 gene putative promoter and ORF revealed Ad54 was the closest to Ad type 8.

Conclusion: The propagation of Ad54 in A549 is slow compared with Ad37, Ad64 and Ad5. Slow propagation could have been caused by slow genomic replication resulting from delayed viral entry or E1 transcription initiation. The EKC caused by Ad54 needs more attention because the slow propagation of Ad54 may contribute to prolonged disease duration.

Keywords: adenovirus, epidemic keratoconjunctivitis, species D, type 54, slow propagation.

Introduction

Human mastadenovirus (Ad) is a DNA virus that infects various organs throughout the body [1]. Ad has a linear, double stranded DNA genome, approximately 35 kb in size [2]. Over 100 types of Ad, including serotypes and genotypes, are known (http://hadvwg.gmu.edu/), and they belong to seven species (Ad A to G) [2].

Among them, several members of Ad D species: Ad type 8 (Ad8), 37 (Ad37), 54 (Ad54), and 64 (formerly known as 19a) (Ad64) are responsible primarily for causing epidemic keratoconjunctivitis (EKC). The ocular manifestations caused by the member of Ad D viruses are more severe than those caused by Ad B (Ad type 3, 7), C: Ad type 2, 5(Ad5), and E: (Ad type 4), which cause mild follicular conjunctivitis and pharyngoconjunctival fever [3]. Thus, typing Ad isolated from eye samples can predict the clinical course of the subsequent infection.

Recently, a number of recombinant Ad types have been identified and reported [4–7], including Ad54, first reported as an Ad8 mutant in 2008 [8]. From 2015 to 2018, Ad54 caused nationwide outbreak and was the most frequently detected Ad type in eyes of patients with EKC in Japan (https://nesid4g.mhlw.go.jp/Byogentai/Pdf/data41j.pdf), furthermore, this type was found only in Japan until 2017 [9]. Globally, Ad8 is the main pathogen of EKC, whereas in Japan its detection has declined [10], where Ad54 has become the primary EKC type. No other viruses detected in patients with severe EKC have exhibited a detection rate as

high as that of Ad54 for 4 years consistently. Motivated by this epidemiological observation, we investigated the viral characteristics of Ad54.

Species D reportedly exhibits slower reductions in the viral genome after infection [3] and the high viral loads of Ad54 in clinical samples were reported as maintained over a long period of time following disease onset [11]. As a feature of virus isolation from clinical samples, Akiyoshi, et al. [12], Nakamura, et al. [13], and Kaneko, et al. [14] report that Ad54 detection is difficult and time-consuming. However, these three reports used only clinical samples which contained viral loads variously for virus isolation, while quantitative experiments could not be performed. Therefore, we conducted the quantitative analysis to make the same amount of viruses to inoculate in A549 cells and attempted to elucidate the reason for the difficulty of virus isolation with Ad54 compared with those of Ad37 and Ad64, the major forms of EKC in Japan, and used Ad5 as control.

Materials and methods

Viral strain and cell lines

Prototype strains of Ad5 and Ad37 were obtained from the American Type Culture Collection (ATCC) (Manassas). Ad54 and Ad64, as reported previously, were obtained from the

75 Adenovirus Reference Center (the National Institute of Infectious Diseases; NIID) [15, 16].
76 The strains were grown in A549 cells (CCL-185, ATCC) with Minimum Essential Medium
77 Eagle with Earle's salts (Eagle's MEM, Sigma-Aldrich Japan) supplemented with 5% fetal
78 bovine serum (Biowest), 1% L-Alanine/L-Glutamine (200 mmol/L) (Wako Pure Chemical
79 Industries (Wako)), 0.2% gentamicin sulfate solution (50 mg/ml) (Wako), and 0.1%
80 amphotericin B (Wako) in 25 cm^2 tissue culture flask (TPP. After a 100% cytopathic effects
81 (CPE) was detected and subjected to two freeze-thaw cycles, the cells with medium were
82 collected in a 15 mL conical centrifuge tube. The tube was centrifuged at 1,500 ×g for two
83 minutes. The supernatant was collected in a new conical centrifuge tube, and 5% fetal bovine
84 serum was added to make a total volume of 10 ml. Each 500 µl of the supernatant was stored
85 as viral stock at −80°C. All experiments described here were performed at NIID, an approved
86 facility equipped for experiments with viral infections. This study was not subject to ethical
87 review because it did not use clinical specimens or patient information.
88
89 **Observation of CPE**
90
91 A total of 50 µL of virus, containing 1.0×10^5 copies/µL, was inoculated into 24 wells of
92 confluent A549 cell monolayers. The inoculated cells were maintained in 450 µL of 5%
93 Eagle's MEM and incubated under an atmosphere of 5% CO_2 (ASTEC CO. Ltd.). We added

500 μL of 5% Eagle's MEM to the control wells. The cultures were daily observed over seven days for the appearance of CPE. Each time the cells were observed, we took photographs using a phase-contrast microscope (Wraymer) to examine for CPE. Each experimental condition was analyzed using three wells.

Measurement of the number of adenoviral genome copies

After the virus was harvested, we collected cell pellets and supernatant from each well at 6 h, 1, 2, 3, 4, 5, 6, and 7 days post-infection (dpi) (Fig. 1). First, 250 μL of the culture supernatant was sucked by a pipette into a 1.5-mL micro-centrifuge tube "A." Tube A was centrifuged at 1,500×g for 5 minutes, and then 200 μL supernatant was collected into a new 1.5 mL micro-centrifuge tube "B." The cells that remained in the well were carefully scraped with a cell scraper (TPP) and collected into tube A. We poured 500 μL D-PBS (Wako) into the same well to wash the scraper and well, and then the wash solution was collected in tube A. Tube A was centrifuged at 1500×g for 5 minutes, and the supernatant was discarded. Tube A was preserved as a pellet tube and tube B as a supernatant tube at −80°C until DNA extraction.

Before DNA extraction, tube A pellets were mixed well by vortexing with 200 μL D-PBS. Tube B contents were used without any further processing. Viral DNA was extracted from 200 μL of each sample using the High Pure Viral Nucleic Acid Kit (Roche). We stored

113 the extracted 100 μL of viral DNA at −80°C until PCR. The number of adenoviral genome
114 copies per microliter of pellets was determined using quantitative real-time PCR (qPCR)
115 following a previously described method [14] and the pharyngoconjunctival fever/EKC
116 Diagnostic Manual, 3rd Edition (National Institute of Infectious Diseases,
117 https://www.niid.go.jp/niid/images/lab-manual/adeno_v3.pdf). Briefly, 2 μL of template DNA
118 was added to 18 μL in total containing 10 μL of 2× SYBR Premix Ex *Taq* II (Takara bio), 0.4
119 μL of 50 × Rox Reference dye II (Takara bio), 0.16 μL of 50 μM concentration of the primers
120 Hex 3 and Hex 4 (Supplemental Table), and 7.28 μL of DW. Real-time PCR was performed
121 using the StepOne real-time PCR system (ABI) (StepOne). The cycling conditions included
122 an initial denaturation step at 95°C for 1 min, followed by 40 cycles of denaturation at 95°C
123 for 5 s, annealing, and extending at 60°C for 30 s. All experiments were repeated three times.
124
125 **Virus titration**
126
127 Ad virus titers were determined using micro titer plates by three-fold serial dilution of viral
128 stock and inoculation with 100 μL of dilution into each of the 96 wells (TPP) containing a
129 monolayer of A549 cells. Plates were incubated at 34°C with 5% CO_2 and observed daily for
130 CPE for seven days. The Spearman–Karber's method was used to calculate the median tissue
131 culture infective dose ($TCID_{50}$)/ml [17]. All tests were repeated three times.

Calculation of Ads growth rate

To compare the speed of viral propagation, growth rate was defined as the intracellular genomic gain of Ad, considered to represent genomic replication in the A549 cells before viral shedding into culture supernatant. The time point just before the virus was released into the supernatant was determined, and then, a straight line was drawn between two additional points: (1) the viral load at that point and (2) the viral load in pellets at 6 h. Specifically, we extracted viral loads in pellets at 6 h and 2 dpi for Ad5, 37, and 64 (Fig. 3A). For Ad54, viral loads in pellets were extracted at 6 h and on 3 dpi. Growth rate was calculated from the slope of the straight line as per the previous study [18]: Growth rate = Δ log viral load / Δ time. Statistical analyses (n = 3) were performed using one-way analysis of variance (ANOVA) followed by Tukey–Kramer post hoc test using Microsoft Excel 2011 (Microsoft) and Statcel4 add-in software (OMS). A p-value <0.05 was considered statistically significant.

The expression levels of early transcription factor E1 gene per infected cell

To synthesize cDNA, PrimeScript RT reagent Kit and gDNA Eraser Kit (Takara bio) were used for reverse transcriptions of mRNA and removal of genomic DNA (gDNA). Briefly, 7

μL of total viral DNA from pellets, 2 μL of 5 × gDNA eraser buffer, and 1 μL of gDNA Eraser were mixed to form a total reaction volume of 10 μL. This solution was incubated at 42°C for 2 min to eliminate the gDNA. Ten microliters of reverse-transcription reaction mixture, 4 μL of 5 × PrimeScript Buffer 2, 1 μL of PrimeScript RT Enzyme Mix 1, 1 μL of Oligo dT Primer (50uM) (Takara bio), and 4 μL of RNase Free dH_2O were combined and incubated at 37°C for 15 min, followed by 85°C for 5 s, to generate cDNA using a PCR Thermal Cycler Dice (Takara bio). Eighty microliters of TE (pH 8.0) (Wako) were added to cDNA to make a total volume of 100 μL, stored at −20°C until use. The qPCR was performed using a StepOne and SYBR Premix Ex *Taq* II (Takara bio). Thermocycling was performed in a final volume of 20 μL containing 2 μL of the cDNA sample, 10 μL of 2 × SYBR Premix Ex *Taq* II, 0.4 μL of 50 × Rox Reference dye II, and 0.8 μL of 10 μM concentration of the each E1 primer (forward and reverse), and 6 μL of distilled water. The E1 primers for qPCR were designed by Primer Express Software v2.0 (ABI). All primers were checked for amplification efficiency, and only primers with equal amplification efficiencies were used in the experiments. PCR amplification was performed using a StepOne, and the cycling conditions were 95°C for 1 min and 40 cycles of 95°C for 5 s and 60°C for 30 s. To account for the number of infected cells per well, the RNase P gene (one copy of which is present in human genomic DNA) was quantified using the ABI TaqMan RNase P Detection Reagents Kit (Thermo Fisher Scientific) and Probe qPCR Mix (Takara bio) on a StepOne. Reactions were

prepared using 10 μL of Probe qPCR Mix, 1 μL of 20 × RNase P Primer-Probe, 0.4 μL of Rox reference dye, 2 μL of viral DNA of pellets, and 6.6 μL of distilled water. Cycling conditions were 95°C for 20 s and 40 cycles of 95°C for 1 s and 60°C for 20 s. A series of 2 serial dilutions of human genomic DNA containing the Kit was used in duplicate to produce the standard curve. The expression levels of E1 gene per infected cell were calculated according to the formula $2^{-(Ct)}$/ the number of cells, which were calculated from RNase P. Each experimental condition was analyzed in three wells and repeated three times. Statistical analyses were performed using ANOVA followed by Tukey–Kramer post hoc test using Microsoft Excel 2011 with Statcel4 add-in software. A p-value of <0.05 was considered statistically significant.

Phylogenetic analysis of the region including promoter of E1 gene and E1 open reading frame (ORF)

To investigate growth rate delays and E1 expression in Ad54, we compared the E1 upstream sequence, including putative E1 promoter and regulator, and ORF of E1 in Ad related to EKC and Ad5. The genome sequences of Ad5 (AY339865.1), Ad37 (AB448775.1), Ad54 (AB333801.2), Ad64 (JQ326307.1), Ad type 8 (Ad8: AB448767.1), and Ad type 56 (Ad56: HM770721.2) were obtained from a public database (GenBank: https:

189 //www.ncbi.nlm.nih.gov/nuccore.). The multiple alignments and phylogenetic tree analysis
190 were performed using MEGA 6.0 software (https://www.megasoftware.net/). DNA sequences
191 were aligned using the ClustalW program (http://www.ebi.ac.uk/clustalw/) with an open gap
192 penalty of 15, a gap extension penalty of 6.66, a transition weight of 0.5 with IUB DNA
193 weight matrix, and a delay divergent cutoff of 30%. The neighbor-joining method was used
194 for phylogenetic tree analysis, the reliability of which was assessed by bootstrap resampling
195 (1,000 pseudo-replicates). Kimura's 2-parameter method was used to calculate genetic
196 distance [19].
197
198 **Results**
199
200 **Viral replication comparisons**
201
202 **CPE**
203 Fig. 2 depicts CPE induced by Ads. Each of the A549 cells infected with Ad5, 37, and 64
204 became enlarged, rounded, and were highly refractile on the third dpi. By 4 dpi, they
205 aggregated into irregular clusters on the well plate bottoms (Fig. 2). A day later, all the cells
206 dispersed from the well plate bottoms and were observed floating in the culture medium. The
207 Ad54 infected cells began to swell on 4 dpi, and clear CPE was confirmed on 5 dpi. Ad5, 37,

and 64 cells all floated within 24 h, and Ad54 floated within 48 h. Compared to the other types, Ad54 required more dpi (time) for confirmation of CPE. No CPE was observed in the negative control.

Comparisons of viral loads of Ad genomic DNAs and $TCID_{50}$

We separately compared the viral loads of Ad genomic DNAs in pellets of A549 cells and supernatant. On 1 dpi, Ad5, 37, and 64 copies increased in the pellets by ~100-fold. The viral copies of these three Ads reached ~10,000-fold (maximum) from initial viral loads within 3 dpi (Fig. 3A). On 2 dpi, Ad5, 37, and 64 exhibited viral shedding into the culture supernatant (Fig. 3B). On 2 dpi, the Ad54 viral load in cultured cells reached was ~100-fold of inoculation levels and reached ~10,000-fold of inoculation levels on 6 dpi; however, the levels failed to plateau (maximum) within 7 days. Clear virus shedding into the supernatant was observed on 3 dpi. Compared to the cells infected with other Ads, the viral loading of Ad54 was slower both in the pellets and in supernatant. Table 1 shows the relationships between the viral loads of Ad genomic DNA and $TCID_{50}$. $TCID_{50}$ had the lowest viral loads in Ad54.

Comparison of Ad growth

Intracellular genomic gains occurred on 2 dpi for Ad5, 37, and 64 and on 3 dpi for Ad54 (Fig. 3B). The growth rates displayed in Table 2 were calculated using the formula shown in the Methods section. Significant changes in growth rate were observed between Ad54 and the

other D types ($p < 0.01$). No significant differences were found between Ad37 and Ad64. The growth rate of Ad54 was significantly lower than those of other types.

Confirmation of E1 gene expression (Fig. 4)

Relative expression levels of the Ad54 E1 gene were significantly lower than cells infected with other Ads on 1 dpi and gradually increased on 2 dpi and 3 dpi.

Phylogenetic analysis of the E1 gene putative promoter and ORF

DNA sequences of types Ad37 and 64 were phylogenetically closest for both the putative promoter and ORF of the E1 gene. Ad54 was the closest to Ad8. Ad5 was the phylogenetically farthest from Ad54 (Figs. 5A, B).

Discussion

There are no comparative reports with accurate quantification on the propagation of Ad54 , therefore, we compared the phenotypic proliferative properties of Ad37, 54, and 64, which are the major causes of EKC in Japan. Although Ad8 is a major EKC pathogen globally, it was not included except for the phylogenetic analysis. This was because: (1) the prototype

246 strain of Ad8 provided by ATCC was contaminated with Ad type 10 [20] and (2) Ad8 strains
247 may have differences in their propagation speeds among strains [21–23]. The hypothesis
248 about Ad8 strains should be clarified in another paper. To date, no differences in viral
249 propagation among strains, such as Ad8, have been observed in Ad54. A549 was used as the
250 most sensitive cells to isolate Ads, including Ad54 [12, 24, 25]. We inoculated the same
251 amount of each Ad virus at the beginning and separately compared Ad viral loads in pellets
252 with supernatant, the latter was assumed to contain the complete Ad virions [26].
253 Our results produced five major characteristics of Ad54. First, the initiation of CPE
254 and the time required until all the cells show CPE in Ad54 were delayed compared with other
255 Ads (Fig. 2). Second, viral load in pellets and viral shedding in supernatant were slower for
256 Ad54 than for the other types (Figs. 3 a, b, c). Third, the growth rate of Ad54, indicated by
257 intracellular genomic gain, was significantly slower than the other types (Table 2). Fourth, the
258 relationship between Ad54 genomic DNA viral loads and $TCID_{50}$ was the lowest among the
259 tested types (Table 1). Last, Ad54 was the lowest level on 1 dpi, according to the expression
260 level of the E1 gene per infected cell, which acts as an indirect measure of viral entry (Fig. 4).
261 Slower viral propagation of Ad54 could be (at least partly) due to slow E1
262 expression or slowing of the steps that precede E1 expression. In other words, Ad54 could
263 experience defects during any of the early steps of viral replication: virus adsorption, entry, or
264 E1 gene initiation [27]. Because we detected approximately 10^5 copies/well of Ad54 DNA

from the pellet at 6 h after infection, the virus may have been able to adsorb to the host cells. Notably, there was some lag between viral entry and E1 gene transcription initiation in Ad54. We were unable to prove the existence of any defects in viral entry of Ad54. However, assuming no viral entry issues, the delayed E1 gene transcription initiation might have resulted from an E1 gene putative promoter or the ORF of the E1 gene itself.

E1 gene expression is directly linked to the growth rate. Therefore, we investigated phylogenetic differences among the Ad viruses for E1 gene promotion. Four complete sequences of Ad54 (AB333801, LC215446, LC215427, and LC215423) were obtained from the NCBI database. The upstream region of E1 and E1 ORF were identical among the strains. The putative promoter and ORF of the Ad54 E1 gene were phylogenetically closest to Ad8 (Fig. 5). Ad54 is considered phylogenetically derived from Ad8 [28, 29]. We could not investigate Ad8 in this study; however, the growth rate of Ad8 may be slow [21, 23]. This prediction is consistent with the results of previous reports, in which Ad8 could not be isolated from clinical samples [13, 14].

Our results indicate that the slow propagation of Ad54 could have been caused by slow genomic replication resulting from delayed viral entry or E1 transcription initiation that induced an overall delay in genome replication. Slow propagation might be the reason owing to which the viral load did not peak within 7dpi for Ad54.

283 Because viral replication in Ad54 was delayed, the latent period may be longer than
284 the typical 8–10 days [30]. Additionally, slow propagation of Ad54 might have prolonged the
285 duration of infection. Furthermore, species D reportedly exhibits slower reductions in the
286 viral genome after infection [2]. Therefore, Ad54 appeared to take long from latency to
287 termination of infection than the other types. Extended duration of the disease can lead to an
288 increase in the chance of infecting others, likely spreading the infection. There is currently no
289 effective treatment for EKC, and when nosocomial infections or a major epidemic occur, the
290 resultant social and economic losses can be substantial [31, 32].
291 Limitation of this study: we used only A549 cells, believed to be the most sensitive
292 cell line for Ads. To verify whether these experimental results can be applied to conjunctival
293 epithelial cells *in vitro* and *in vivo*, additional quantitative experiments are required in the
294 future. The experiment for the viral propagation should be performed in the near future for
295 other EKC types of Ad, including prototype Ad8 and recent isolates, such as Ad8, Ad53,
296 Ad56, etc. Because expression level analysis and cell observation imaging were not
297 conducted by sorting only infected cells, the correlation between the expression level of E1
298 and CPE after the virus entered the cell could not be proved in this study. Infection
299 experiments after cell synchronization will be necessary in the future.
300 The slower propagation of Ad54 compared to the other Ads was confirmed kinetically
301 in this study. The results of this study might provide clues to the development of specialized

302 countermeasures for each Ad type. Ads are highly contagious and considering that high viral
303 loads are maintained at infection onset [11], more attention is required to prevent the spread
304 of Ad54.

305 **Acknowledgements** The authors would like to thank Enago (www.enago.jp) for the
306 English language review. This study was partly supported by a Ministry of Health, Labor and
307 Welfare Grant-in-Aid for Scientific Research (10110713). This is a post-peer-review, pre-
308 copyedit version of an article published in Japanese Journal of Ophthalmology. The final
309 authenticated version is available online at: https://doi.org/10.1007/s10384-020-00727-2.

310 **Conflicts of interest** T. Tsukahara-Kawamura, None; N. Hanaoka, None; T. Fujimoto, None;
311 M. Konagaya, None; E. Uchio, None.

312

313 **References**

314 1. White DO, Fenner FJ. Adenoviridae. In: Medical Virology. 4th ed. San Diego: Academic
315 Press; 1994. pp. 306–16.
316 2. Robinson CM, Singh G, Lee JY, Dehghan S, Rajaiya J, Liu EB, et al. Molecular evolution
317 of human adenoviruses. Sci Rep. 2013;3:1812.
318 3. Lee CS, Lee AY, Akileswaran L, Stroman D, Najafi-Tago K, Kleiboeker S, et al.
319 Determinants of outcomes of adenoviral keratoconjunctivitis. Ophthalmology.
320 2018;125:1344-53.

4. Walsh MP, Chintakuntlawar A, Robinson CM, Madisch I, Harrach B, Hudson NR, et al. Evidence of molecular evolution driven by recombination events influencing tropism in a novel human adenovirus that causes epidemic keratoconjunctivitis. PLoS One. 2009;4:e5635.
5. Hashimoto S, Gonzalez G, Harada S, Oosako H, Hanaoka N, Hinokuma R, et al. Recombinant type Human mastadenovirus D85 associated with epidemic keratoconjunctivitis since 2015 in Japan. J Med Virol. 2018;90:881-9.
6. Espínola EE, Barrios JC, Russomando G, Mirazo S, Arbiza J. Computational analysis of a species D human adenovirus provides evidence of a novel virus. J Gen Virol. 2017;98:2810-20.
7. Kaján GL, Kajon AE, Pinto AC, Bartha D, Arnberg N. The complete genome sequence of human adenovirus 84, a highly recombinant new Human mastadenovirus D type with a unique fiber gene. Virus Res. 2017;242:79-84.
8. Ishiko H, Shimada Y, Konno T, Hayashi A, Ohguchi T, Tagawa Y, et al. Novel human adenovirus causing nosocomial epidemic keratoconjunctivitis. J Clin Microbiol. 2008;46:2002-8.
9. Balasopoulou A, Kokkinos P, Pagoulatos D, Plotas P, Makri OE, Georgakopoulos CD, et al. A molecular epidemiological analysis of adenoviruses from excess conjunctivitis cases. BMC Ophthalmol. 2017;17:51.

10. Fujimoto T, Matsushima Y, Shimizu H, Ishimaru Y, Kano A, Nakajima E, et al. A molecular epidemiologic study of human adenovirus type 8 isolates causing epidemic keratoconjunctivitis in Kawasaki City, Japan in 2011. Japanese Journal of Infectious Diseases. 2012;65:260-3.

11. Uemura T, Migita H, Ueno T, Tsukahara-Kawamura T, Saeki Y, Fujimoto T, et al. Clinical and virological analysis of epidemic keratoconjunctivitis caused by adenovirus type 54 in a regional ophthalmic clinic in Kyushu, Japan. Clin Ophthalmol. 2018;12:511-7.

12. Infectious Agents Surveillance Report. Infectious Disease Surveillance Center, Japan. IASR. 2008;29:346-7. (in Japanese)

13. Nakamura N, Hirano E, Kowada K, Ishiguro F, Yamagishi Z, Adhikary AK, et al. Surveillance of adenovirus D in patients with epidemic keratoconjunctivitis from Fukui prefecture, Japan, 1995-2010. J Med Virol. 2012;84:81-6.

14. Kaneko H, Suzutani T, Aoki K, Kitaichi N, Ishida S, Ishiko H, et al. Epidemiological and virological features of epidemic keratoconjunctivitis due to new human adenovirus type 54 in Japan. Br J Ophthalmol. 2011;95:32-6.

15. Fujimoto T, Hanaoka N, Konagaya M, Kobayashi M, Nakagawa H, Hatano H, et al. Evaluation of a silver-amplified immunochromatography kit for adenoviral conjunctivitis. J Med Virology. 2019;91:1030-5.

16. Zhou X, Robinson CM, Rajaiya J, Dehghan S, Seto D, Jones MS, et al. Analysis of human adenovirus type 19 associated with epidemic keratoconjunctivitis and its reclassification as adenovirus type 64. Invest Ophthalmol Vis Sci. 2012;53:2804-11.

17. Lorenz RJ, Bogel K. Methods of calculation: The Spearman-Karber method. WHO Monograph Series. 1973;23:321-9.

18. Atabani SF, Smith C, Atkinson C, Aldridge RW, Rodriguez-Peralvarez M, Rolando N, et al. Cytomegalovirus replication kinetics in solid organ transplant recipients managed by preemptive therapy. Am J Transplant. 2012;12:2457-64.

19. Kimura M. A simple method for estimating evolutionary rates of base substitutions through comparative studies of nucleotide sequences. J Mol Evol. 1980;16:111-20.

20. Yamane S, Lee AW, Hanaoka N, Gonzalez G, Kaneko H, Ishida S, et al. Identification of contamination in the American Type Culture Collection stock of human adenovirus type 8 by whole-genome sequencing. J Virol. 2013;87:1285-6.

21. Wigand R. Pitfalls in the identification of adenoviruses. J Virol Methods. 1987;16:161-9.

22. Guo DF, Shinagawa M, Aoki K, Sawada H, Itakura S, Sato G. Genome typing of adenovirus strains isolated from conjunctivitis in Japan, Australia, and the Philippines. Microbiol Immunol. 1988;32:1107-18.

23. Adhikary AK, Ushijima H, Fujimoto T. Human adenovirus type 8 genome typing. J Med Microbiol. 2012; 61:1491-503.

24. Enomoto M, Fujimoto T, Konagaya M, Hanaoka N, Chikahira M, Taniguchi K, et al. Cultivation for 21 days should be considered to isolate respiratory adenoviruses from samples containing small numbers of adenoviral genomes. Jpn J Infect Dis. 2010;63:338-41.

25. Akiyoshi K, Suga T, Fukui K, Taniguchi K, Okabe N, Fujimoto T. Outbreak of epidemic keratoconjunctivitis caused by adenovirus type 54 in a nursery school in Kobe City, Japan in 2008. Jpn J Infect Dis. 2011;64:353-4.

26. Badr KR, Parente-Rocha JA, Baeza LC, Ficcadori FS, Souza M, Soares CM, et al. Quantitative proteomic analysis of A549 cells infected with human adenovirus Type 2. J Med Virol. 2019;91:1239-49.

27. Yin J, Redovich J. Kinetic modeling of virus growth in cells. Microbiol Mol Biol Rev. 2018;82:e00066-17.

28. Kaneko H, Aoki K, Ohno S, Ishiko H, Fujimoto T, Kikuchi M, et al. Complete genome analysis of a novel intertypic recombinant human adenovirus causing epidemic keratoconjunctivitis in Japan. J Clin Microbiol. 2011;49:484-90.

29. Gonzalez G, Yawata N, Aoki K, Kitaichi N. Challenges in management of epidemic keratoconjunctivitis with emerging recombinant human adenoviruses. J Clin Virol. 2019;112:1-9.

30. Hierholzer, J.C. Adenoviruses. In: Lennette E.H. et al., editors. Diagnostic procedures for

viral, rickettsial and chlamydial infections. 7th ed. Washington, DC: American Public Health Association; 1995. pp. 169-88.

31. Udeh BL, Schneider JE, Ohsfeldt RL. Cost effectiveness of a point-of-care test for adenoviral conjunctivitis. Am J Med Sci. 2008;336**:**254-64.

32. Piednoir E, Bureau-Chalot F, Merle C, Gotzamanis A, Wuibout J, Bajolet O. Direct costs associated with a nosocomial outbreak of adenoviral conjunctivitis infection in a long-term care institution. Am J Infect Control. 2002;30:407-10.

Figure legends

Fig. 1 Methods of collecting cell pellets and supernatant. First, 250 μL of the culture supernatant was sucked by a pipette into a 1.5 mL micro-centrifuge tube A. A was centrifuged at 1,500×g for 5 minutes, and then 200 μL supernatant was collected into a new 1.5 mL micro-centrifuge tube B. The cells that remained in the well were carefully scraped with a cell scraper and collected in tube A. We poured 500 μL D-PBS into the same well to wash the scraper and well, and then the wash solution was collected in tube A. Tube A was centrifuged at 1500×g for 5 minutes, and the supernatant was discarded. Tube A was preserved as a pellet tube and tube B as a supernatant tube within a −80°C refrigerator until DNA extraction

Fig. 2 Cytopathic effects (CPE) of Human mastadenoviruses (Ads) on each day post-infection (dpi). CPEs induced by Ad5, 37, 64, and 54 were photographed using a phase-contrast microscope on 3, 4, 5, and 6 dpi (original magnification, ×200). The cells became enlarged, rounded, and highly refractile in the early stages of CPE. After that, they aggregated into irregular clusters, gathering on the bottoms of well plates (arrows) on 3 dpi for Ad5, 37, and 64. On the other hand, in Ad54, the cell began to swell on 4 dpi, and the clear CPE was recognized on 5 dpi. All the cells floated within 24 h for HAdV5, 37, and 64. Ad 54 required 48 h to develop the same kind of microscopic features. The initiation of CPE and the time required until all the cells were impacted by CPE in Ad54 were delayed compared with the other Ads. CPE was not observed in the negative control. N, negative control; Ad, Human mastadenovirus; dpi, Days post-infection. Scale bar: 50 μm

Fig. 3 The amount of Ads DNA copies and growth rate. The amount of Ads DNA copies in pellets (a), supernatant (b), and total (c) per well post-infection. The viral copies increased ~10,000-fold (maximum) within 3 dpi (a). Viral shedding of Ad5, 37, and 64 into the culture supernatant was observed on 2 dpi (b). On the other hand, the viral load of Ad54 in pellets reached ~100-fold of the inoculation levels on 2 dpi, reaching ~10,000-fold by 6 dpi. Ad54 exhibited slower viral load increases compared to the other Ad (c). Standard deviations of

433 triplicate assays at each time point are indicated by error bars. Abbreviations; Ad, Human
434 mastadenovirus; Dpi, Days post-infection.
435
436 **Fig. 4** The E1 gene expression level. mRNA of E1 gene serves as an indirect measure of viral
437 entry for each Human mastadenovirus type 5 (Ad5), 37 (Ad37), 54 (Ad54), 64 (Ad64), and
438 negative control (N), as detected by quantitative real-time PCR on 1, 2, and 3 dpi. The
439 relative E1 gene expression level for Ad54 was significantly lower compared with that of the
440 other Ads on 1 dpi and gradually increased on 2 and 3 dpi. The standard deviations for each
441 time point of the triplicate assays are indicated by error bars. *Significant differences ($p <$
442 0.05) between Ad54 and all the other Ads by one-way ANOVA followed by the Tukey–
443 Kramer post hoc test. Abbreviations: Ad, Human mastadenovirus; N, negative control; N.D.,
444 not detected; Dpi, Days post-infection
445
446 **Fig. 5** Delayed E1 gene transcription initiation Phylogenetic analysis of the E1 upstream
447 region and E1 open reading frame (ORF)
448 Phylogenetic tree of (a) the upstream region, including the E1 putative promoter and
449 regulator and (b) E1 gene among Ads related to EKC. Types Ad37 and 64 were the closest
450 matches and were compared as predictors of Ad54. Ad54 was the closest to Ad8. Ad5 was,

phylogenetically, the farthest from Ad54. The scale bar shows the number of base substitutions per site.

* The length of upstream region is as follows: Ad5:559bp, Ad8:563bp, Ad37:569bp, Ad54:568bp, Ad56:571bp, and Ad64:569bp.

The Ad5 E1 ORF includes several introns and region from 560 to 1545 in AY339865.1. (986bp). The Ad8 E1: ORF includes several introns and region from 564 to 1420 in AY339865.1. (857bp). The Ad37 E1: ORF includes several introns and region from 570 to 1426 in AB448775.1. (857bp). The Ad54 E1: ORF includes several introns and region from 569 to 1425 in AB333801.2. (857bp). The Ad56 E1: ORF includes several introns and region from 572 to 1422 in HM770721.2. (851bp). The Ad64 E1: ORF includes several introns and region from 570 to 1426 in JQ326207.1. (857bp). Abbreviations; Ad, Human mastadenovirus

Table 1 The relationship between viral loads of Ad genomic DNAs and $TCID_{50}$

Ad type	$TCID_{50}$ /ml at 10^5 copies / μL	Ratio of $TCID_{50}$ /ml at 10^5 copies / μL*
Ad5	1.54×10^5	12
Ad37	1.87×10^5	14
Ad54	1.31×10^4	1
Ad64	3.43×10^4	3

Abbreviations: Ad, Human mastadenovirus; $TCID_{50}$, the median tissue culture infective dose.

*The ratio of $TCID_{50}$/ml was calculated by setting the $TCID_{50}$/ml value at 10^5 copies/μL of Ad54 to 1.

473 **Table 2** Growth rate of each Ads

Ad5	Ad37	Ad54	Ad64
0.11*	0.09*	0.05	0.09*

Abbreviations: Ad, Human mastadenovirus.

*Significant differences ($p < 0.05$) between Ad54 and all the other Ads by one-way ANOVA followed by the Tukey–Kramer post hoc test.

474

475

476

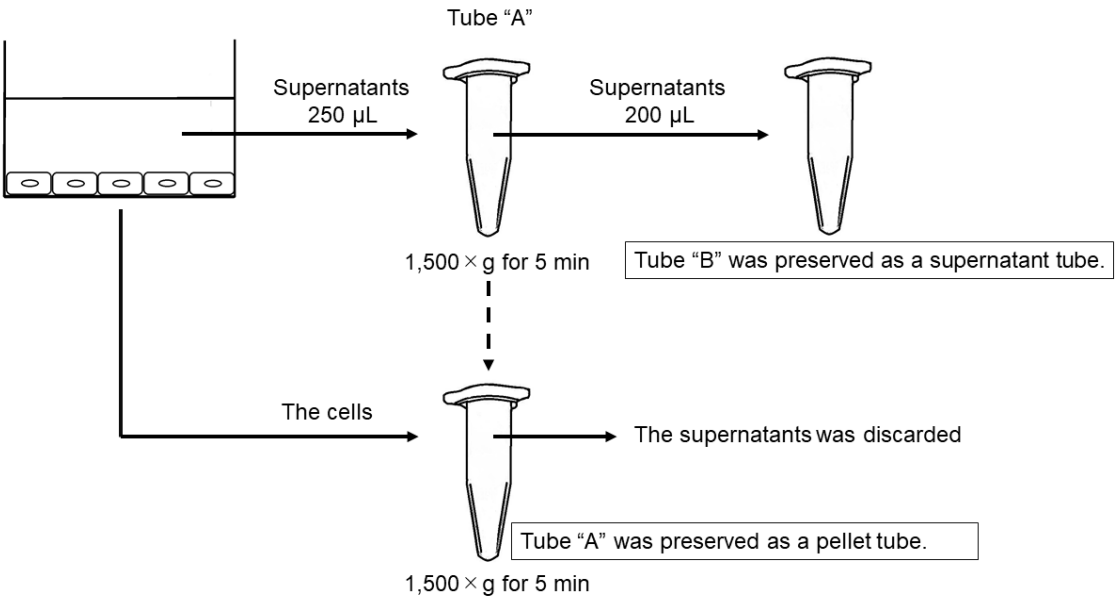

477 Fig. 1

478

479

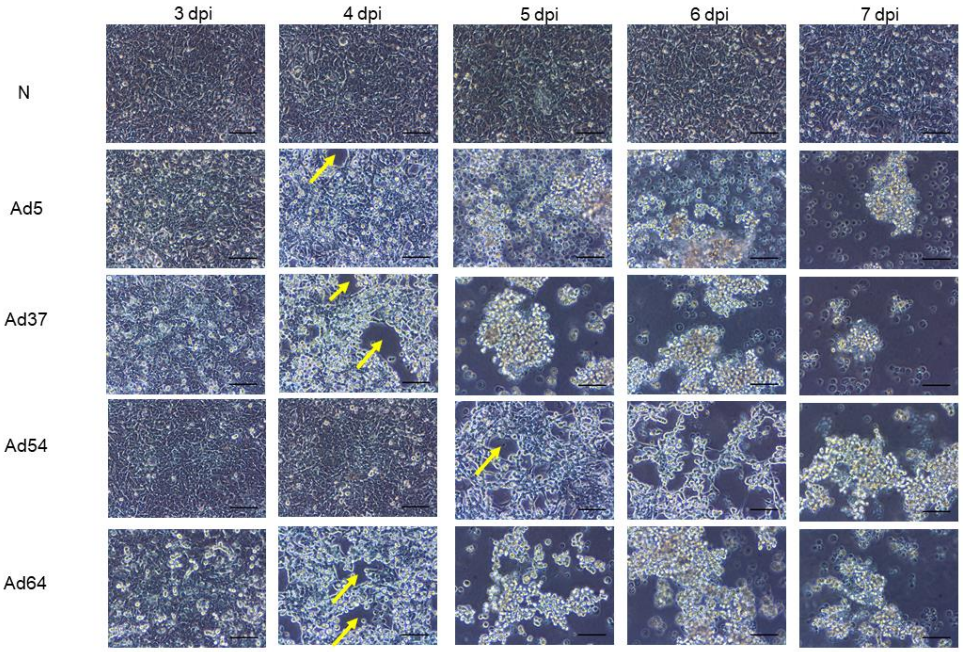

480 Fig. 2

481

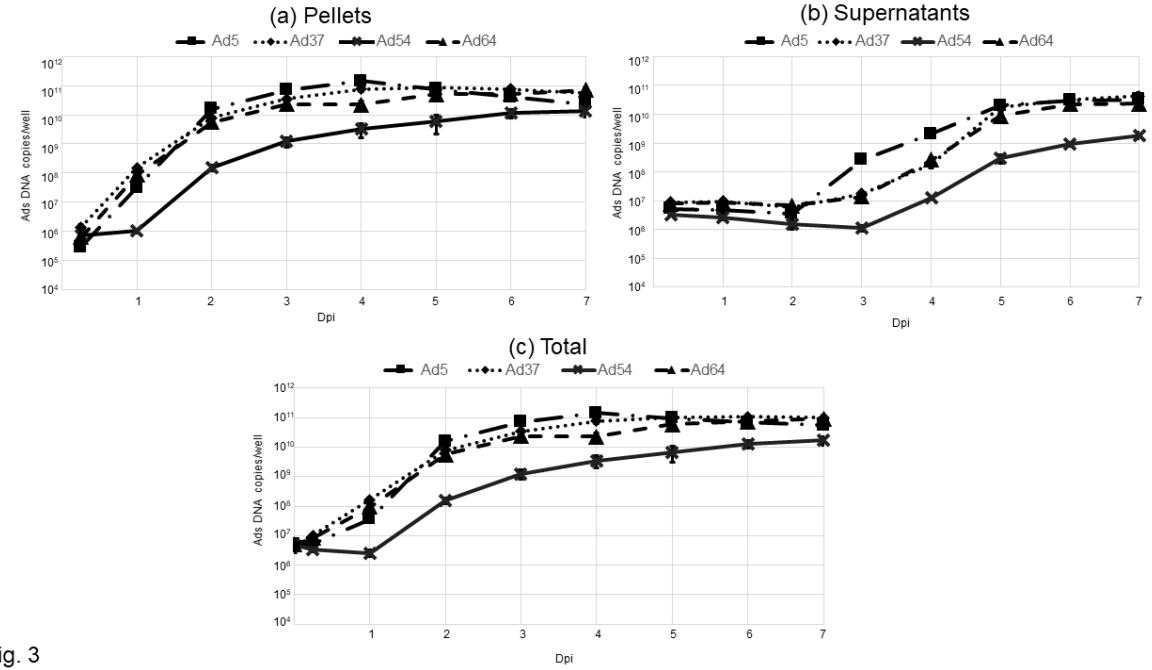

482 Fig. 3

483

484

485

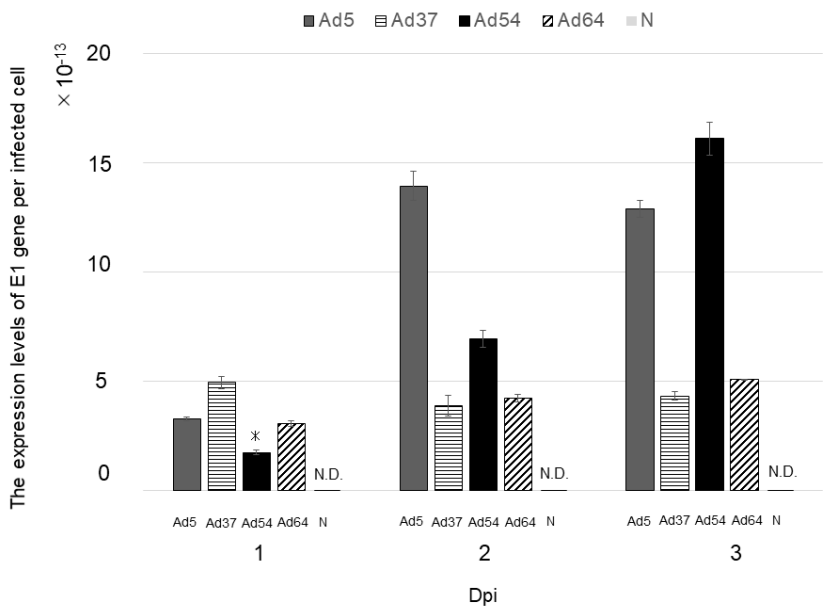
Ad5
Ad37
Ad54
Ad64
N
The expression levels of E1 gene per infected cell
× 10-13
20
15
10
5
0
N.D.
N.D.
N.D.
Ad5 Ad37 Ad54 Ad64 N
Ad5 Ad37 Ad54 Ad64 N
Ad5 Ad37 Ad54 Ad64 N
1
2
3
Dpi

Fig. 4

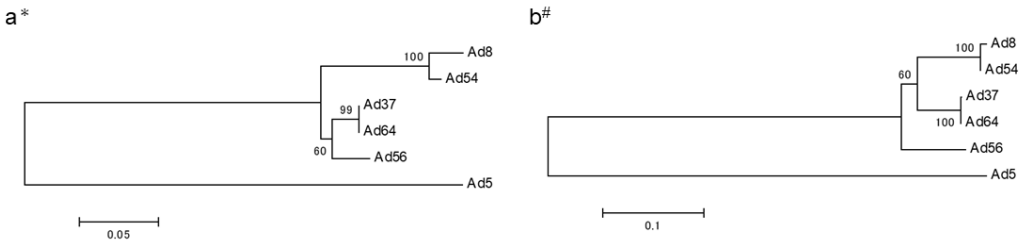
a*
100
Ad8
Ad54
99
Ad37
Ad64
60
Ad56
Ad5
0.05
b#
100
Ad8
Ad54
60
Ad37
100
Ad64
Ad56
Ad5
0.1

Fig. 5

Supplemental Table. The primers used in this study.

Primer name	Nucleotide sequence (5'–3')	Target region	Reference
Hex3	GACATGACTTTCGAGGTCGATCCCATGGA	Ad5, 37, 64 hexon 3	Fujimoto T, et al.[15]
Hex4	CCGGCTGAGAAGGGTGTGCGCAGGTA	Ad5, 37, 64 hexon 4	
Hex3-Ad54	GACATGACCTTTGAGGTGGACCCCATGGA	Ad54 hexon 3	
Hex4-Ad54	CCGGCGGAGAAGGGCGTGCGCAGGTA	Ad54 hexon 4	
Ad5_E1F	CCAACGAGGAGGCGGTTT	Ad5 E1	This study
Ad5_E1R	TCCTGCACCGCCAACAT		
Ad54_E1_F	AATGACACGCCCCTGCAA	Ad54 E1	This study
Ad54_E1_R	TCTCGCCACTCGGTCTAACC		
Ad37, 64_E1_F	CCGGGCAAGGCTGTAGATC	Ad37, 64 E1	This study
Ad37, 64_E1_R	GCGTTTGTGTCTCCGGTCTT		

Ad, human mastadenovirus